PHYSICAL REVIEW D **86,** 065028 (2012)

Testing 3 + 1 and 3 + 2 neutrino mass models with cosmology and short baseline experiments

Maria Archidiacono,[1] Nicolao Fornengo,[2] Carlo Giunti,[2] and Alessandro Melchiorri[1]
[1]*Physics Department, Università di Roma "La Sapienza" and INFN, P.le Aldo Moro 2, Rome 00185, Italy*
[2]*Department of Physics, University of Torino and INFN, Via P. Giuria 1, Torino I-10125, Italy*
(Received 1 August 2012; published 25 September 2012)

Recent results from short-baseline neutrino oscillation experiments suggest the presence of additional sterile neutrinos, while cosmic microwave background anisotropy measurements point toward an excess of radiation, which could in fact be provided by light sterile neutrino states. In this paper we properly combine these two data sets (short-baseline and cosmic microwave background) to derive bounds on the sterile neutrino masses in the 3 + 1 and 3 + 2 schemes, finding a potentially good agreement between the two data sets. However, when data on galaxy clustering are further included in the analysis, a tension between the oscillation and cosmological data is clearly present. From our combined global analysis the allowed 95% C.L. mass intervals for the additional sterile neutrino states are: 0.85 eV $< m_4 <$ 1.18 eV for the 3 + 1 scheme, and $m_4 <$ 0.70 eV and 0.67 eV $< m_5 <$ 1.35 eV for the 3 + 2 scheme.

DOI: 10.1103/PhysRevD.86.065028 PACS numbers: 14.60.Pq, 14.60.St, 98.80.−k, 98.80.Es

I. INTRODUCTION

In recent years, the impressive experimental discoveries in two fields of investigation, namely neutrino physics and cosmic microwave background (CMB) anisotropies, have revolutionized our knowledge in particle physics and cosmology. Neutrino oscillations experiments have not only firmly established that neutrino are massive and mixed particles (for reviews, see e.g., Refs. [1–3]), but have also provided precise measurements of the three-neutrino mixing parameters (see the recent global fits in Refs. [4,5]). On the other hand, the measurements of the angular spectrum of the CMB anisotropies (see e.g., Ref. [6]) have not only fully confirmed the expectations of the standard cosmological scenario but also provided a precise determination of most of its parameters. Moreover, with the continuous experimental improvements, a clear interplay between neutrino physics and cosmology is emerging. Neutrinos are indeed a fundamental energy component in modern cosmology. A cosmological neutrino background is expected in the standard model and affects both the shape of the CMB and the formation of cosmological structures (see e.g., Ref. [7]). The recent cosmological data have provided a clear evidence (more than 5 standard deviations) for the existence of the primordial neutrino background and have strongly constrained the absolute neutrino mass scale (see e.g., Ref. [8]).

However, the measurements of CMB anisotropies made by the Atacama Cosmology Telescope [9] and South Pole Telescope[10] experiments, when combined with the measurements of the Hubble constant H_0 and galaxy clustering data, have provided interesting hints for an *extra* relativistic weakly interacting component, coined dark radiation. Parametrizing this energy component with the effective number of neutrino species $N_{\rm eff}$, the recent data bound it to $N_{\rm eff} = 4.08 \pm 0.8$ at 95% C.L. (see e.g., Refs. [11–13]), whereas the standard prediction for only three active neutrino species is $N_{\rm eff} = 3.046$ [14]. While this result should be taken with some grain of salt since it is derived from a combination of cosmological data and some tension does exist between the data (see e.g., Ref. [15]), it is anyway interesting since a fourth or fifth neutrino species seems also suggested by short-baseline (SBL) oscillation experiments. The appearance and disappearance data of several SBL experiments can be explained by the mixing of the three active neutrinos with one or two additional sterile neutrinos in the so-called 3 + 1 and 3 + 2 models (see Refs. [16–21]).

This work is therefore aimed to determine the masses of the sterile neutrinos in 3 + 1 and 3 + 2 models using data from SBL experiments and recent cosmological data and check if the results are mutually compatible. Finally, we combine the bounds from the two different analyses to have a joint probability for the masses of sterile neutrinos. Previous analyses discussing the interplay between SBL and cosmological data may be found in Refs. [22–25]. We also notice here that bounds on extra radiation from big bang nucleosynthesis (BBN) [23,25–27] may be quite severe, pointing toward a more constrained value for $N_{\rm eff}$ than what is implied by CMB data. Recent analyses on BBN constraints are indicating a favored value of $N_{\rm eff}$ smaller than 4 [26]. This result would imply that the 3 + 2 scheme might be already considered as disfavored by BBN data.

The paper is organized as follows: in Secs. II and III we present the data sets we make use of, the method we adopt to analyze them and the results we obtain regarding the SBL experiments and in the cosmological context, respectively; in Sec. IV the joint analysis method and results are shown; finally we summarize our conclusions in Sec. V.

II. NEUTRINO OSCILLATIONS ANALYSIS

The SBL neutrino oscillation analysis is performed following Refs. [17–19].

We consider 3 + 1 and 3 + 2 neutrino spectra in which ν_e, ν_μ, ν_τ are mainly mixed with ν_1, ν_2, ν_3, whose masses are much smaller than 1 eV and there are one or two additional massive neutrinos ν_4 and ν_5 which are mainly sterile and have masses of the order of 1 eV. Short-baseline oscillations are generated by the large squared-mass differences Δm^2_{41} and Δm^2_{51}, with

$$\Delta m^2_{51} \geq \Delta m^2_{41} \gg \Delta m^2_{31} \gg \Delta m^2_{21}. \quad (1)$$

The small squared-mass differences Δm^2_{21} and Δm^2_{31} which generate, respectively, solar and atmospheric neutrino oscillations (see Refs. [1–3]) have negligible effects in SBL oscillations and are ignored in the following. The two heavy neutrino masses m_4 and m_5 which are probed by cosmological data are simply connected to the squared-mass differences relevant for SBL oscillations by

$$m_4 \simeq \sqrt{\Delta m^2_{41}}, \qquad m_5 \simeq \sqrt{\Delta m^2_{51}}. \quad (2)$$

We fit the data set of SBL neutrino oscillation experiments corresponding to the GLO-HIG analysis in Ref. [19], in which the low-energy MiniBooNE neutrino [28] and antineutrino [29–31] data corresponding to the so-called "MiniBooNE low-energy anomaly" are not considered since they induce a strong tension between appearance and disappearance data (see the discussions in Refs. [18,19]). We made the following two improvements with respect to the analysis presented in Ref. [19]:

(1) We used the reactor neutrino fluxes presented in the recent white paper on light sterile neutrinos [32], which update Refs. [33,34]. The new fluxes are about 1.3% larger than those we used before, which were taken from the reactor antineutrino anomaly publication [35].

(2) We replaced the KamLAND bound on $|U_{e4}|^2$ with a more powerful constraint obtained from solar neutrino data [36–38]. Taking into account the recent measurement of $|U_{e3}|^2$ in the Daya Bay [39] and RENO [40] reactor neutrino experiments ($|U_{e3}|^2 = \sin^2\vartheta_{13} = 0.025 \pm 0.004$), from Fig. 1 of Ref. [38] we inferred the approximate upper bound $|U_{e4}|^2 = \sin^2\vartheta_{14} \lesssim 0.02$ at 1σ (see Ref. [41]).

In our analysis of SBL neutrino oscillation data we apply first the standard χ^2 method. The minimum value of χ^2, the number of degrees of freedom, the goodness-of-fit and the corresponding best-fit values of the oscillation parameters are presented in Table I. The results concerning the 3 + 1 and 3 + 2 fits are similar to those reported, respectively, in Ref. [19] for the GLO-HIG case and Ref. [17], with small variations due to the consideration of different data sets. From Table I we can see that in both the 3 + 1 and 3 + 2 frameworks the global goodness-of-fit is satisfactory.

The allowed regions of Δm^2_{41} versus the effective SBL oscillation amplitudes $\sin^2 2\vartheta_{e\mu}$, $\sin^2 2\vartheta_{ee}$ and $\sin^2 2\vartheta_{\mu\mu}$ (with $\sin^2 2\vartheta_{\alpha\beta} = 4|U_{\alpha 4}|^2|U_{\beta 4}|^2$) are shown in Fig. 1.

TABLE I. Values of $\chi^2_{\rm min}$, number of degrees of freedom (NDF), goodness-of-fit (GoF) and best-fit values of the mixing parameters obtained in our 3 + 1 and 3 + 2 fits of short-baseline oscillation data.

	3 + 1	**3 + 2**
$\chi^2_{\rm min}$	142.1	134.1
NDF	138	134
GoF	39%	48%
Δm^2_{41}[eV^2]	1.62	0.89
$\lvert U_{e4}\rvert^2$	0.035	0.018
$\lvert U_{\mu 4}\rvert^2$	0.0086	0.015
Δm^2_{51}[eV^2]		1.61
$\lvert U_{e5}\rvert^2$		0.022
$\lvert U_{\mu 5}\rvert^2$		0.0047
η		1.57π

These regions are relevant, respectively, for $\overset{(-)}{\nu}_\mu \leftrightarrows \overset{(-)}{\nu}_e$, $\overset{(-)}{\nu}_e \to \overset{(-)}{\nu}_e$ and $\overset{(-)}{\nu}_\mu \to \overset{(-)}{\nu}_\mu$ oscillation experiments. They are more similar to those shown in Fig. 3 of Ref. [19] than the region presented in Ref. [41] because the larger reactor antineutrino fluxes used in this analysis increase the reactor antineutrino anomaly, leading to a larger value of $|U_{e4}|^2$, which tends to cancel the effect of the solar neutrino constraint.

The allowed regions in the Δm^2_{41}-Δm^2_{51} plane obtained in the 3 + 2 analysis are shown in Fig. 2. One can see that the allowed regions are similar to those presented in Fig. 9 of Ref. [17], with small variations due to the different considered data sets.

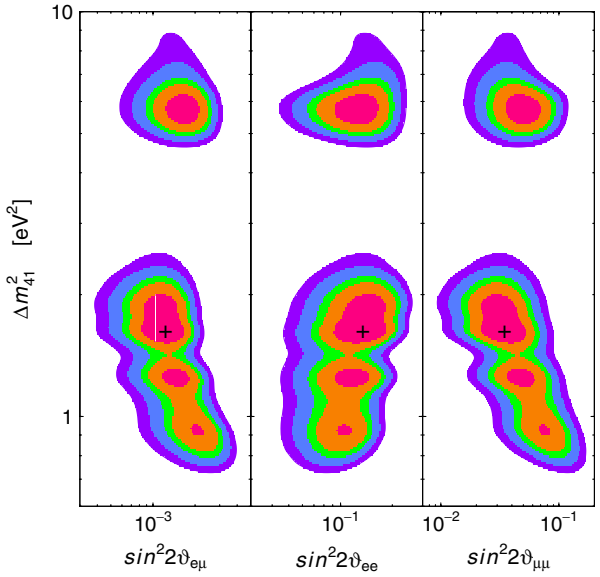

FIG. 1 (color online). Allowed regions in the $\sin^2 2\vartheta_{e\mu} - \Delta m^2_{41}$, $\sin^2 2\vartheta_{ee} - \Delta m^2_{41}$ and $\sin^2 2\vartheta_{\mu\mu} - \Delta m^2_{41}$ planes obtained from the global fit of short-baseline neutrino oscillation data in the 3 + 1 scheme using the standard χ^2 method. The best-fit point is indicated by a cross (see Table I).

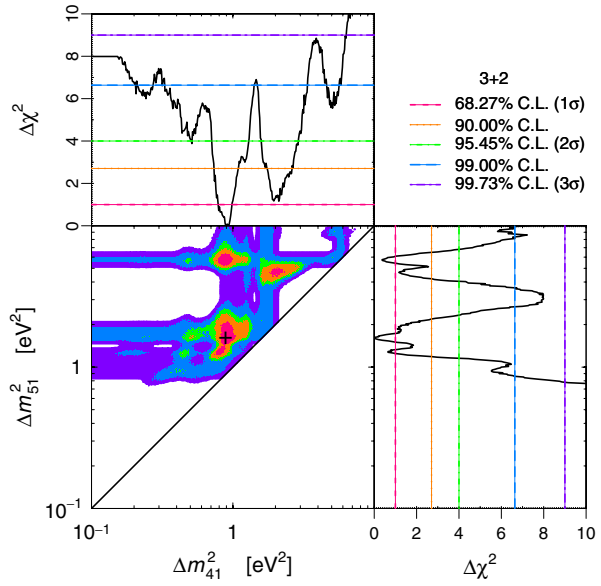

FIG. 2 (color online). Allowed regions in the Δm^2_{41}-Δm^2_{51} plane and corresponding marginal $\Delta\chi^2$'s obtained from the global fit of short-baseline neutrino oscillation data in 3 + 2 schemes using the standard χ^2 method. The best-fit point is indicated by a cross (see Table I).

Since we want to perform a combined analysis of SBL oscillation data and cosmological data, and the cosmological analysis is performed with the Bayesian method, we have also analyzed the SBL oscillation data with a Bayesian approach. We assumed the sampling distribution of the data D:

$$p(D|\theta_M, M) \propto e^{-\chi^2(D,\theta_M)/2}, \tag{3}$$

where M is the model ($M = 3 + 1$ or $M = 3 + 2$), θ_M is the corresponding set of oscillation parameters (listed in Table I) and $\chi^2(D, \theta_M)$ is the corresponding χ^2 function. The sampling probability is called "likelihood" when considered as a function of the parameters of the model.

In each of the two models, we calculated the posterior probability distribution of the oscillation parameters using Bayes' theorem:

$$p(\theta_M|D, M) = \frac{p(D|\theta_M, M)p(\theta_M|M)}{p(D|M)}, \tag{4}$$

where $p(D|M)$ is easily calculated as a normalization constant. We assumed a flat prior distribution in the logarithmic space of the oscillation parameters, except for the CP-violating phase η in the 3 + 2 spectrum (see Ref. [17]) for which we used a linear scale in the interval $[0, 2\pi]$. For $\log(\Delta m^2_{41}/\mathrm{eV}^2)$ and $\log(\Delta m^2_{51}/\mathrm{eV}^2)$ we considered the range $[-1, 1]$. For $\log|U_{e4}|^2$, $\log|U_{\mu 4}|^2$, $\log|U_{e5}|^2$, $\log|U_{\mu 5}|^2$ we considered the range $[-4, 0]$.

Since we are interested in combining the results of the analysis of SBL oscillation data with that of the cosmological data, where the only shared parameters are the neutrino masses in Eq. (2), we calculated the marginal posterior probability distributions of the squared-mass differences by integrating the posterior probability distribution over the other oscillation parameters taking into account the scale of the flat prior. For example, in the 3 + 1 model:

$$\begin{aligned} &p(\log\Delta m^2_{41}|D, 3 + 1) \\ &\quad = \int d\log|U_{e4}|^2 d\log|U_{\mu 4}|^2 p(\log(\Delta m^2_{41}), \\ &\qquad \log|U_{e4}|^2, \log|U_{\mu 4}|^2|D, 3 + 1). \end{aligned} \tag{5}$$

In this way, we obtained the posterior probability distribution of Δm^2_{41} in the 3 + 1 spectrum plotted in Fig. 3 (thick green line exhibiting several sharp peaks) and the allowed regions in the Δm^2_{41}-Δm^2_{51} of the 3 + 2 spectrum shown in Fig. 4. Comparing with Fig. 2, one can see that the Bayesian allowed regions are wider than those obtained with the χ^2 method. The difference is due to the different method of marginalization with respect to the other mixing

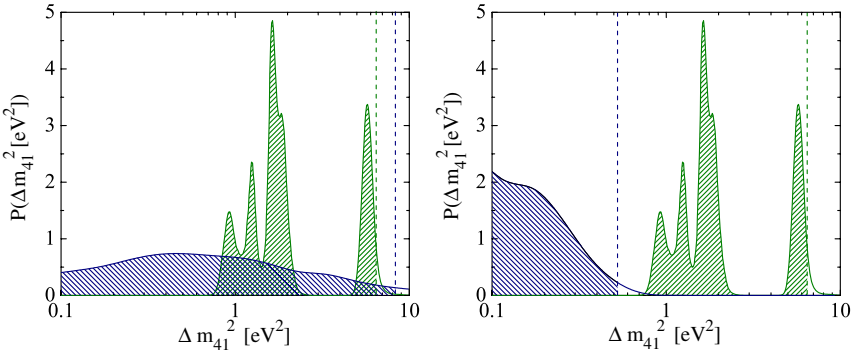

FIG. 3 (color online). Marginal posterior probabilities obtained with a Bayesian analysis for Δm^2_{41} in the 3 + 1 scheme. The thick (green) solid line exhibiting several sharp peaks (the same in the two panels) refers to the analysis of the short-baseline oscillation data alone. The blue line exhibiting a broad peak stands for the analysis of the cosmological data alone: CMB-only data for the left panel, CMB data implemented with SDSS and HST information for the right panel. In all cases, the shaded regions refer to the 95% coverage of the probability distribution.

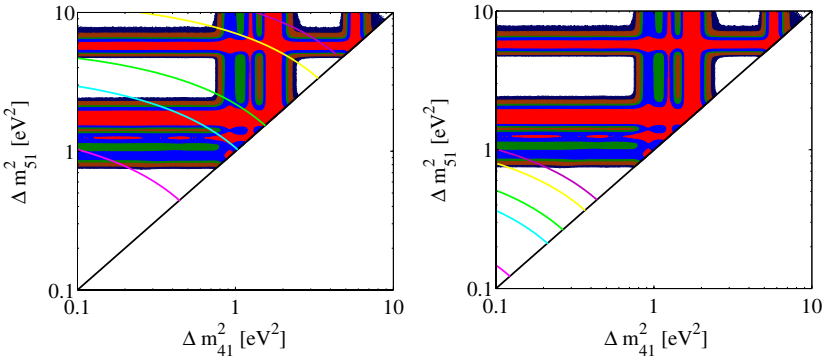

FIG. 4 (color online). Allowed regions in the Δm^2_{41}-Δm^2_{51} plane obtained with a Bayesian analysis. The "boxy" regions (the same in the two panels) refer to the global analysis of the short-baseline oscillation data and are relative to the following confidence levels (from the innermost to the outermost region): 68.27% (red), 90.00% (light blue), 95.45% (green), 99.00% (brown) and 99.73% (dark blue). The arc-shaped solid lines refer to the analysis of the cosmological data: the left panel stands for the CMB-only data set, while the right panel refers to the inclusion of the SDSS information and HST prior to the CMB data. The different lines refer to the following confidence levels (from the lower curve to the upper curve, in each panel): 68.27, 90.00, 95.45, 99.00 and 99.73%.

parameters (mixing angles and *CP*-violating phase): in the χ^2 method one considers only the minimum of the χ^2 in the range of each marginalized parameter, whereas in the Bayesian method one must integrate the posterior probability density over the marginalized parameter space. Since the data do not constrain much the values of the marginalized parameters (see Figs. 10–12 of Ref. [17]), the Bayesian integration gives significantly different results from the χ^2 marginalization. The allowed vertical bands with constant value of Δm^2_{41} are due to the fact that one can have a comparable fit for any value of Δm^2_{51} and negligible $|U_{e5}|$ and $|U_{\mu 5}|$, which is effectively equivalent to a 3 + 1 framework. The same applies to the allowed horizontal bands with constant value of Δm^2_{51}.

III. COSMOLOGICAL ANALYSIS

The cosmological analysis is performed in two different steps: first by analyzing CMB-only data and then by further adding data from large scale structure and priors on the Hubble parameter. The CMB analysis is performed by employing the following data sets: WMAP7 [6], Atacama Cosmology Telescope [9] and South Pole Telescope [10]. The large scale structure analysis makes use of information on dark matter clustering from the matter power spectrum extracted from the SDSS-DR7 luminous red galaxy sample [42]. Finally, the Hubble parameter prior we use is based on the latest Hubble Space Telescope observations [43].

We analyze data sets up to $\ell_{\rm max} = 3000$. The analysis method we adopt is based on the publicly available Markov Chain Monte Carlo (MCMC) package CosmoMC [44] with a convergence diagnostic done through the Gelman and Rubin statistic.

We sample the following six-dimensional standard set of cosmological parameters, adopting flat priors on them: the baryon and cold dark matter densities $\Omega_{\rm b}h^2$ and $\Omega_{\rm c}h^2$, the ratio of the sound horizon to the angular diameter distance at decoupling θ, the optical depth to reionization τ, the scalar spectral index n_S and the overall normalization of the spectrum A_S. We account for foregrounds contributions including three extra amplitudes: the Sunyaev-Z'eldovich amplitude, the amplitude of clustered point sources and the amplitude of Poisson distributed point sources. We consider purely adiabatic initial conditions and we impose spatial flatness. In this work both active and sterile neutrinos are assumed to be fully thermalized. Sterile neutrino thermalization [45–49] is realized through oscillations and occurs if the mass splittings and mixing angles with active neutrinos are not too small. An approximate condition is that the relevant squared-mass separation Δm^2 and effective mixing $\sin\theta$ satisfy the following requirement [48]:

$$\Delta m^2 \sin^4\theta > 3 \times 10^{-6}\ \text{eV}^2. \tag{6}$$

For the 3 + 1 case, this condition is always fulfilled, as can be seen in Fig. 2. In the 3 + 2 case, the situation is more complex, since the allowed regions from the SBL analysis may extend to the case where one of the two additional neutrinos has very small values of the mixing angle and/or the mass splitting, as is shown in the analysis of Ref. [17]. The situation where one of the two sterile neutrinos decouples (and the 3 + 1 scheme is actually recovered as a limit) is a possible solution for the 3 + 2 case. Table I above and Ref. [17] show that for the best-fit parameters the values of the mass splittings and effective mixing angles are sufficient to ensure thermalization of both states in the 3 + 2 case; when the parameters are moved toward the edges of the their allowed ranges, Eq. (6) may not be satisfied for both sterile states and full thermalization of one of the two extra neutrinos may not occur and a dedicated analysis of the thermalization process would be required. In our analysis we assume that full thermalization always occurs in the allowed parameter space. Clearly, a partial or nonstandard thermalization could lead to completely different constraints on the sterile neutrino mass [45–48]. In particular, Ref. [48] shows that in the

nonthermal case the cosmological energy density in sterile neutrinos does not monotonically increase with the mass and it is constrained to be less then 0.003 at 95% C.L. for masses >1 eV; as an aftermath, in the matter power spectrum the suppression due to free streaming is smaller at higher masses. This effect can relax the constraints on the sterile neutrino masses around 1 eV.

The aim of this paper is to specifically test 3 + 1 and 3 + 2 neutrino mass models by means of a joint analysis of both cosmological and SBL experiments data. Therefore, contrary to the typical approach (see e.g., Refs. [24,25,50]), in the cosmological analysis we do not let the effective number of relativistic degrees of freedom $N_{\rm eff}$ to vary as a free parameter; instead we fix it at the values $N_{\rm eff} = 3 + 1$ or $N_{\rm eff} = 3 + 2$ for the 3 + 1 and 3 + 2 schemes, respectively. This is consistent with the assumptions done in the oscillation analysis and with the hypothesis of cosmological full thermalization of all neutrino states (including the sterile ones; see the recent discussions in Refs. [45,46]). Consistently to the analysis of Sec. II, we fix the three active neutrinos to be massless and we allow the sterile neutrinos to have masses which vary as additional free parameters. Since we are interested to sample the joint sensitivity of cosmological and SBL neutrino data on the sterile-neutrinos mass parameters, in the cosmological analysis we do not employ the neutrino mass fraction f_ν (as it is usually done), but instead we sample directly $\log\Delta m^2_{41}$ and $\log\Delta m^2_{51}$. This implies a flat prior on those parameters.

Before attempting a joint analysis with the SBL data, which have been presented in the previous section, we report in Table II the constraints on the cosmological parameters using CMB-only data and CMB data plus Sloan Digital Sky Survey (SDSS) information together with the Hubble Space Telescope (HST) prior, and assuming a 3 + 1 model with three massless active neutrinos and one massive sterile neutrino; and a 3 + 2 model with three massless active neutrinos plus two massive sterile neutrinos. The 95% C.L. mass bounds on the sterile neutrinos is 2.88 eV for the 3 + 1 scheme, while for the 3 + 2 model the bound on the sum of the masses of the two additional sterile neutrinos is 2.48 eV, both of them share a 2σ upper limit of about 1.24 eV, when CMB-only data are used. These bounds drastically improve when also SDSS data and the HST prior are included in the analysis (see Ref. [51]), reaching the value of 0.73 eV for the 3 + 1 case and about 1 eV for the 3 + 2 case. Both the 3 + 1 and 3 + 2 schemes are statistically well acceptable, with no noticeable preference in the minimal χ^2. The only visible (and expected) difference between the 3 + 1 and 3 + 2 schemes is that two additional neutrinos require a larger value of the dark matter abundance $\Omega_c h^2$ to compensate a delay of the equivalence time, which would instead be induced by the presence of an additional light degree of freedom in the 3 + 2 case [23]. The correction due to nondegeneracy between the mass of the first and the second sterile neutrino in the 3 + 2 model is of the order of precision of present numerical codes and so undetectable using only the present cosmological data (CMB and matter power spectra). Moreover, the degeneracies with other cosmological parameters make the detection of the neutrino mass differences impossible at the state of the art (see Ref. [52]).

Figure 3 shows the marginal posterior probability of the cosmological Bayesian analysis for the 3 + 1 case, compared with the results of the SBL study. The blue line exhibiting a broad peak stands for the analysis of the cosmological data alone and the left panel refers to CMB-only data, while the right panel refers to the CMB data implemented with SDSS and HST information. The two panels of the figure show how the inclusion of SDSS and HST information is relevant to set the more stringent constraint on the cosmological upper bound on the neutrino mass. The shaded regions refer to the 95% C.L. coverage of the probability distribution, from which the bounds on m_4 of Table II are derived. When compared with the SBL analysis and its 95% C.L. mass intervals (three slightly discontinued ranges in the interval

TABLE II. MCMC estimation of the cosmological parameters from the analysis of CMB-only data and from CMB data plus matter power spectrum information (SDSS) and a prior on H_0 (HST), in the case of three massless active neutrinos and one massive sterile neutrino (3 + 1 scheme) and assuming three massless active neutrinos plus two massive sterile neutrinos (3 + 2 scheme). Neutrino mass upper bounds are reported at the 95% C.L., unless for the 3 + 2 CMB + SDSS + HST case where we quote the best-fit value together with the 68% (95%) C.L. interval.

	3 + 1 CMB only	**3 + 2** CMB only	**3 + 1** CMB + SDSS + HST	**3 + 2** CMB + SDSS + HST
$\Omega_b h^2$	0.0224 ± 0.0004	0.0226 ± 0.0004	0.0224 ± 0.0004	0.0226 ± 0.0004
$\Omega_c h^2$	0.135 ± 0.007	0.156 ± 0.009	0.133 ± 0.004	0.156 ± 0.004
τ	0.085 ± 0.014	0.087 ± 0.015	0.084 ± 0.014	0.086 ± 0.014
H_0	71.5 ± 3.6	73.6 ± 4.4	73.1 ± 1.6	74.6 ± 2.0
n_s	0.970 ± 0.015	0.985 ± 0.016	0.977 ± 0.010	0.990 ± 0.010
$\log(10^{10}A_s)$	3.21 ± 0.05	3.20 ± 0.05	3.19 ± 0.04	3.19 ± 0.04
$\Sigma m\ (eV)$	<2.88	<2.48	<0.73	$0.58^{+0.12(+0.45)}_{-0.13(-0.42)}$
$\chi^2_{\rm min}$	7529.5	7532.2	7578.5	7581.1

$0.93\ \text{eV} < m_4 < 1.45\ \text{eV}$ and a higher mass range $2.29\ \text{eV} < m_4 < 2.59\ \text{eV}$), with a best fit at $m_4 = 1.27$ eV, we notice that CMB-only and SBL oscillation data are well compatible among them, with a significant overlap of the corresponding 95% C.L. regions. The 95% C.L. cosmological upper bound $m_4 < 2.88$ eV disfavors the higher mass SBL solution, while it is perfectly compatible with the lower SBL mass ranges. The combination of the cosmological and SBL data sets will therefore produce a clean allowed interval, as shown in the next section. Instead, when SDSS and HST information are included in the analysis, SBL oscillations and cosmological data are in tension, with no overlapping 95% C.L.

The analysis for the 3 + 2 scheme is shown in Fig. 4, where C.L. regions in the Δm^2_{41}-Δm^2_{51} plane are reported. The SBL allowed regions clearly show a preference for at least a nonzero neutrino mass (m_5 with our choice of hierarchy in neutrino masses) and a global preference for $m_4 = 0.95$ eV and $m_5 = 1.27$ eV. The cosmological data instead provide upper limits on both sterile neutrino masses, with no clear preference for nonzero values. CMB-only data (left panel) are well compatible with SBL results, with the 95% C.L. upper bound of the cosmological analysis consistent with the corresponding 95% C.L. regions of the SBL analysis and its global best-fit point ($m_4 = 0.95$ eV and $m_5 = 1.27$ eV). Also in the 3 + 2 case, the inclusion of SDSS and HST data produces tension between SBL and cosmological analyses, as is manifest in the right panel of Fig. 4, where only a partial overlap at the 3σ C.L. is present. Figure 4 clearly shows that the whole set of cosmological data will be instrumental in significantly reducing the degeneracy of the allowed solutions of the SBL analysis when the joint analysis will be attempted in the next section.

IV. COMBINED ANALYSIS

The combined analysis of the SBL oscillation data and the cosmological observations has been performed by merging the corresponding posterior probabilities. Since the only relevant parameters common to both sectors are the sterile neutrino masses $m_4 \simeq \sqrt{\Delta m^2_{41}}$ and $m_5 \simeq \sqrt{\Delta m^2_{51}}$ we can define a marginal posterior probability for the joint analysis by directly multiplying the SBL and cosmological marginal posterior probabilities relative to the parameter of interest. For example, in the 3 + 1 case, denoting by $D_{\rm C}$ and $D_{\rm S}$ the cosmological and SBL data we have [53]

$$p(\log\Delta m^2_{41}|D_{\rm C+S}, 3+1) \propto p(\log\Delta m^2_{41}|D_{\rm C}, 3+1) \times p(\log\Delta m^2_{41}|D_{\rm S}, 3+1), \quad (7)$$

where the SBL probability is the one defined in Eq. (5) and the cosmological probability is the one used in the analysis of the previous section and obtained through CosmoMC.

The combined analysis for the 3 + 1 scheme is shown in Fig. 5. As usual, the left panels refers to the case of CMB-only data in the cosmological sector, while the right panel adds SDSS and HST data sets. The horizontal dashed lines identify the credible intervals at 68.27, 90.00, 95.45, 99.00 and 99.73% C.L. In the case of CMB-only data, the inclusion of the cosmological information to the SBL analysis disfavors the higher mass SBL solution around 2.4 eV but maintains the lower mass 95% C.L. allowed intervals ($0.90\ \text{eV} < m_4 < 1.46\ \text{eV}$) and ($2.27\ \text{eV} < m_4 < 2.51\ \text{eV}$) and the best-fit solution ($m_4 = 1.27$ eV). When SDSS and HST information is added to the analysis, the allowed interval of the global analysis shifts down to lower values of the sterile neutrino mass due to the more stringent bound from the cosmological sector. The 95% C.L. mass range becomes $0.85\ \text{eV} < m_4 < 1.18\ \text{eV}$, and the best fit shifts down to $m_4 = 0.93$ eV.

The combined analysis for the 3 + 2 scheme is shown in Fig. 6, again for the case of CMB-only data (left panel) and for the further inclusion of SDSS and HST data (right panel). The global results are that at least one sterile

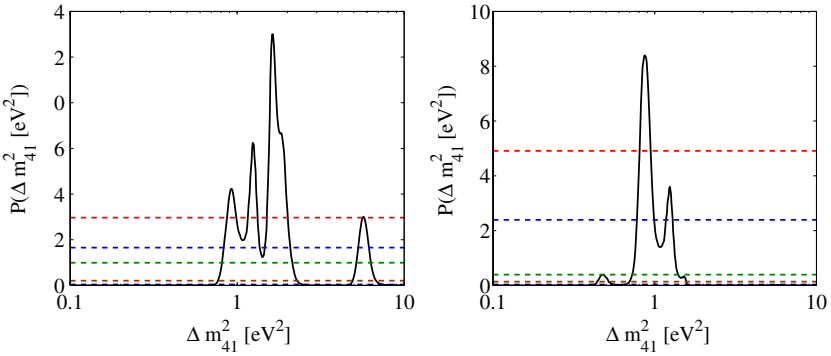

FIG. 5 (color online). Marginal posterior probabilities obtained with a Bayesian analysis for Δm^2_{41} in the 3 + 1 scheme, for the joint analysis of cosmological and short-baseline data. Left panel: the cosmological analysis employs CMB-only data. Right panel: the cosmological analysis adds SDSS and HST information to the CMB data. The horizontal dashed lines identify (from the lower curve to the upper curve, in each panel) the credible intervals at 68.27, 90.00, 95.45, 99.00 and 99.73% C.L.

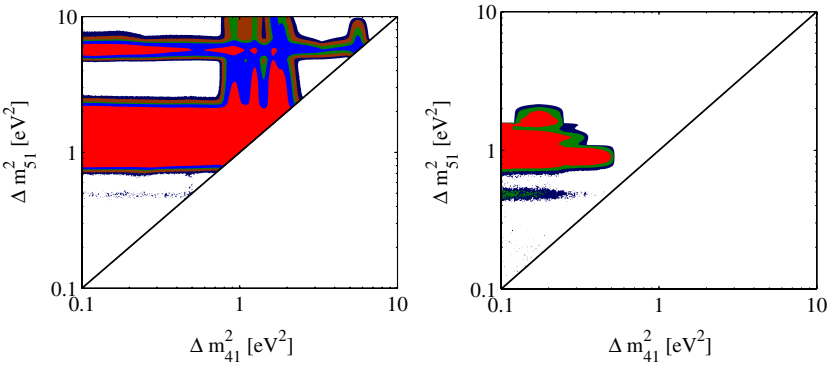

FIG. 6 (color online). Allowed regions in the Δm^2_{41}-Δm^2_{51} plane obtained with a Bayesian approach, for the *joint* analysis of short-baseline and cosmological data. The different regions (as in Fig. 4) refer to the following confidence levels (from the innermost to the outermost region): 68.27% (red), 90.00% (light blue), 95.45% (green), 99.00% (brown) and 99.73% (dark blue). Left panel: SBL data plus the CMB-only data set. Right panel: SBL data plus CMB, SDSS and HST data; in this case only 68.27% (red), 95.45% (green) and 99.73% (dark blue) C.L. are reported.

neutrino needs to be massive, with a mass of the order of 1 eV (m_5 with our choice of hierarchy), while the second sterile neutrino can be massless. The marginalized 95% intervals for the two neutrino masses are $m_4 < 2.51$ eV and $0.86\ \text{eV} < m_5 < 3.16$ eV when CMB-only data are considered; $m_4 < 0.70$ eV and $0.67\ \text{eV} < m_5 < 1.35$ eV for the full analysis which includes also SDSS and HST.

V. CONCLUSIONS

Measuring the number and the mass of sterile neutrinos is one of the most interesting challenges both in cosmology and in neutrino physics. The existing cosmological data indicate that the energy density of the Universe may contain dark radiation composed of one or two sterile neutrinos, which may correspond to those in 3 + 1 or 3 + 2 models which have been invoked for the explanation of SBL neutrino oscillation anomalies. We have performed analyses of the cosmological and SBL data in the frameworks of both the 3 + 1 and 3 + 2 models. Then we have compared the results obtained with the same Bayesian method to figure out if the indications of cosmological and SBL data are compatible.

At the state of the art, cosmological data are sensitive to the sum of neutrino masses for which they give an upper limit at the scale of about 1 eV. Hence they do not allow us to resolve the degeneracy between the mass of the first and the second sterile neutrino in a 3 + 2 model, although in the numerical calculation we leave them as independent parameters. Instead, SBL neutrino oscillations have a completely different parametrization, and in the 3 + 2 model the degeneracy between the two square mass differences Δm^2_{41} and Δm^2_{51} is broken.

The results of our analysis show that the cosmological and SBL data give compatible results when the cosmological analysis takes into account only CMB data. But if the information on the matter power spectrum coming from galaxies surveys are also considered there is a tension between the sterile neutrino masses needed to have SBL neutrino oscillations and the cosmological upper limit on the sum of the masses.

The combined analysis of cosmological and SBL data gives an allowed region for m_4 in the 3 + 1 scheme around 1 eV. In the 3 + 2 scheme, the cosmological data reduce the allowance of the second massive sterile neutrino given by SBL data, leading to a combined fit which prefers the case of only one massive sterile neutrino at the scale of about 1 eV.

In conclusion, our analysis shows that cosmological data are marginally compatible with the existence of one massive sterile neutrino with a mass of about 1 eV, which can explain the anomalies observed in SBL neutrino oscillation experiments. The case of massive sterile neutrinos is less tolerated by cosmological data and in any case the second sterile neutrino must have a mass smaller than about 0.6 eV.

ACKNOWLEDGMENTS

N. F. and C. G. acknowledge the PRIN 2008 research grant "Matter-Antimatter Asymmetry, Dark Matter and Dark Energy in the LHC Era" (MIUR Contract No. PRIN 2008NR3EBK) funded jointly by Ministero dell'Istruzione, dell'Università e della Ricerca (MIUR), by Università di Torino and by Istituto Nazionale di Fisica Nucleare. We acknowledge INFN research Grant No. FA51. N. F. acknowledges support of the Spanish MICINN Consolider Ingenio 2010 Programme under Grant No. MULTIDARK CSD2009-00064 (MICINN). A. M.'s work is supported by PRIN-INAF "Astronomy probes fundamental physics." M. A. acknowledges the European ITN project Invisibles (FP7-PEOPLE-2011-ITN, PITN-GA-2011-289442-INVISIBLES). M. A. thanks the Department of Physics at the University of Turin for hospitality while this research was conducted.

[1] C. Giunti and C. W. Kim, *Fundamentals of Neutrino Physics and Astrophysics* (Oxford University Press, Oxford, England, 2007), ISBN 978-0-19-850871-7.
[2] S. Bilenky, Lect. Notes Phys. **817**, 1 (2010).
[3] Z. Xing and S. Zhou, *Neutrinos in Particle Physics, Astronomy and Cosmology* (Zhejiang University Press, Hangzhou, 2011), ISBN 978-7-308-08024-8.
[4] D. V. Forero, M. Tortola, and J. W. F. Valle, arXiv:1205.4018.
[5] G. L. Fogli, E. Lisi, A. Marrone, D. Montanino, A. Palazzo, and A. M. Rotunno, arXiv:1205.5254.
[6] E. Komatsu *et al.*, Astrophys. J. Suppl. Ser. **192**, 18 (2011).
[7] J. Lesgourgues and S. Pastor, Phys. Rep. **429**, 307 (2006).
[8] S. Hannestad, arXiv:0710.1952.
[9] J. Dunkley *et al.*, Astrophys. J. **739**, 52 (2011).
[10] R. Keisler *et al.*, Astrophys. J. **743**, 28 (2011).
[11] M. Archidiacono, E. Calabrese, and A. Melchiorri, Phys. Rev. D **84**, 123008 (2011).
[12] T. L. Smith, S. Das, and O. Zahn, Phys. Rev. D **85**, 023001 (2012).
[13] J. Hamann, J. Cosmol. Astropart. Phys. 03 (2012) 021.
[14] G. Mangano, G. Miele, S. Pastor, T. Pinto, O. Pisanti, and P. D. Serpico, Nucl. Phys. **B729**, 221 (2005).
[15] E. Calabrese, M. Archidiacono, A. Melchiorri, and B. Ratra, arXiv:1205.6753.
[16] J. Kopp, M. Maltoni, and T. Schwetz, Phys. Rev. Lett. **107**, 091801 (2011).
[17] C. Giunti and M. Laveder, Phys. Rev. D **84**, 073008 (2011).
[18] C. Giunti and M. Laveder, Phys. Rev. D **84**, 093006 (2011).
[19] C. Giunti and M. Laveder, Phys. Lett. B **706**, 200 (2011).
[20] G. Karagiorgi, M. H. Shaevitz, and J. M. Conrad, arXiv:1202.1024.
[21] A. Donini, P. Hernandez, J. Lopez-Pavon, M. Maltoni, and T. Schwetz, J. High Energy Phys. 07 (2012) 161.
[22] A. Melchiorri, O. Mena, S. Palomares-Ruiz, S. Pascoli, A. Slosar, and M. Sorel, J. Cosmol. Astropart. Phys. 01 (2009) 036.
[23] J. Hamann, S. Hannestad, G. G. Raffelt, and Y. Y. Y. Wong, J. Cosmol. Astropart. Phys. 09 (2011) 034.
[24] E. Giusarma, M. Corsi, M. Archidiacono, R. de Putter, A. Melchiorri, O. Mena, and S. Pandolfi, Phys. Rev. D **83**, 115023 (2011).
[25] J. Hamann, S. Hannestad, G. G. Raffelt, I. Tamborra, and Y. Y. Y. Wong, Phys. Rev. Lett. **105**, 181301 (2010).
[26] G. Mangano and P. D. Serpico, Phys. Lett. B **701**, 296 (2011).
[27] F. Iocco, G. Mangano, G. Miele, O. Pisanti, and P. D. Serpico, Phys. Rep. **472**, 1 (2009).
[28] A. A. Aguilar-Arevalo *et al.* (MiniBooNE Collaboration), Phys. Rev. Lett. **102**, 101802 (2009).
[29] A. A. Aguilar-Arevalo *et al.* (MiniBooNE Collaboration), Phys. Rev. Lett. **105**, 181801 (2010).
[30] E. D. Zimmerman (MiniBooNE Collaboration), AIP Conf. Proc. **1441**, 458 (2012).
[31] Z. Djurcic (MiniBooNE Collaboration), arXiv:1201.1519.
[32] K. N. Abazajian *et al.*, arXiv:1204.5379.
[33] T. A. Mueller, D. Lhuillier, M. Fallot, A. Letourneau, S. Cormon, M. Fechner, L. Giot, and T. Lasserre *et al.*, Phys. Rev. C **83**, 054615 (2011).
[34] P. Huber, Phys. Rev. C **84**, 024617 (2011); **85**, 029901(E) (2012).
[35] G. Mention, M. Fechner, T. Lasserre, T. A. Mueller, D. Lhuillier, M. Cribier, and A. Letourneau, Phys. Rev. D **83**, 073006 (2011).
[36] C. Giunti and Y. F. Li, Phys. Rev. D **80**, 113007 (2009).
[37] A. Palazzo, Phys. Rev. D **83**, 113013 (2011).
[38] A. Palazzo, Phys. Rev. D **85**, 077301 (2012).
[39] F. P. An *et al.* (Daya Bay Collaboration), Phys. Rev. Lett. **108**, 171803 (2012).
[40] J. K. Ahn *et al.* (RENO Collaboration), Phys. Rev. Lett. **108**, 191802 (2012).
[41] C. Giunti, LNGS, Assergi, Italy (work in progress).
[42] B. A. Reid, J. N. Chengalur, A. Begum, and I. D. Karachentsev, Mon. Not. R. Astron. Soc. **404**, 60 (2010).
[43] A. G. Riess, L. Macri, S. Casertano, H. Lampeitl, H. C. Ferguson, A. V. Filippenko, S. W. Jha, W. Li, and R. Chornock, Astrophys. J. **730**, 119 (2011).
[44] A. Lewis and S. Bridle, Phys. Rev. D **66**, 103511 (2002).
[45] S. Hannestad, I. Tamborra, and T. Tram, J. Cosmol. Astropart. Phys. 07 (2012) 025.
[46] A. Mirizzi, N. Saviano, G. Miele, and P. D. Serpico, arXiv:1206.1046.
[47] M. A. Acero and J. Lesgourgues, Phys. Rev. D **79**, 045026 (2009).
[48] S. Dodelson, A. Melchiorri, and A. Slosar, Phys. Rev. Lett. **97**, 041301 (2006).
[49] R. Barbieri and A. Dolgov, Nucl. Phys. **B349**, 743 (1991).
[50] M. Archidiacono, E. Giusarma, A. Melchiorri, and O. Mena, arXiv:1206.0109.
[51] M. C. Gonzalez-Garcia, M. Maltoni, and J. Salvado, J. High Energy Phys. 08 (2010) 117.
[52] A. Slosar, Phys. Rev. D **73**, 123501 (2006).
[53] Since we assumed a flat prior for $\theta = \log\Delta m^2_{41}$ in both the SBL and cosmological analyses, using Bayes' theorem (4) we have $p(\theta|D_{\mathrm{C+S}}) \propto p(D_{\mathrm{C+S}}|\theta) = p(D_{\mathrm{C}}|\theta)p(D_{\mathrm{S}}|\theta) \propto p(\theta|D_{\mathrm{C}})p(\theta|D_{\mathrm{S}})$.